Journal of
Materials Chemistry B

Materials for biology and medicine

Accepted Manuscript

This article can be cited before page numbers have been issued, to do this please use: A. M. Bharti, T. T. Chiou, R. K. K. R.K, M. O. Shaikh and C. Chuang, *J. Mater. Chem. B*, 2025, DOI: 10.1039/D5TB00990A.

ROYAL SOCIETY OF CHEMISTRY

rsc.li/materials-b

Multifunctional Au-CNT Nanohybrids for Highly Sensitive Catalytic and Affinity Biosensing Applications

Aditya Manu Bharti[1, 2, #] Terry Ting-Yu Chiou[3, #] R. K. Rakesh Kumar[4,] Muhammad Omar Shaikh[5 *] and Cheng-Hsin Chuang [2 *]

[1]International PhD Program for Science, National Sun Yat-sen University, Kaohsiung 80424, Taiwan.

[2]Institute of Medical Science and Technology, National Sun Yat-sen University, Kaohsiung 80424, Taiwan.

[3]Chung Shan Medical University School of Medicine, Taichung 40201, Taiwan.

[4]Institute of Biomedical Engineering and Nanomedicine, National Healthcare Research institutes, Miaoli County 350, Taiwan.

[5]Sustainability Science and Management Program, Tunghai University, Taichung 407224, Taiwan.

[*] Correspondence Email: omar@thu.edu.tw; Tel.: +886-4-23590121 ext.39204.

[*] Correspondence Email: chchuang@imst.nsysu.edu.tw; Tel.: +886-75-252-000 ext. 7151.

Abstract

Carbon nanotubes (CNTs) possess unique intrinsic properties, such as a huge surface area, homogenous pore size distribution, and nanoscale dimensions, making CNT highly promising for biosensing applications. However, their limited dispersion in biological media and increased resistance hinder efficient charge transfer, necessitating innovative strategies to enhance their performance. This study presents a novel and facile approach for synthesizing multifunctional gold nanoparticle (AuNP)-decorated CNT (Au-CNT) nanohybrids using hetero-functional polyethylene glycol (PEG) as a linker via EDC/NHS chemistry. This approach ensures the covalent and uniform decoration of AuNPs over the surface of CNTs, significantly improving their dispersion, chemical stability, and biocompatibility while preserving their electrochemical activity. Comprehensive morphological, chemical, and electrochemical characterizations confirm improved dispersion and enhanced electron transfer capabilities. To validate its practical application, a proof-of-concept electrochemical sensor is developed for H_2O_2 and glucose detection. Comparative analysis reveals that the Au-CNT nanohybrid exhibits increase in sensitivity over pristine CNTs, demonstrating its superior catalytic performance. These findings highlight the potential of Au-CNT nanohybrids as versatile platforms for advanced electrochemical catalytic and affinity biosensing applications.

Keywords: Carbon nanotubes, Gold nanoparticles, Au-CNT nanohybrid, Biosensing, Bioelectronics.

View Article Online
DOI: 10.1039/D5TB00990A

1. Introduction

Carbon nanotubes have garnered substantial attention due to their intrinsic properties, including uniform pore size distribution, large surface area, and nanoscale dimensions.[1] These unique characteristics make them highly suitable for numerous biomedical applications, including biosensing and bioelectronics. For instance, CNTs are utilized in the development of advanced impedimetric sensors, microelectrodes for neural interfaces, photothermal conversion devices for cancer therapy, printed circuit boards for medical diagnostics, and nanocomposites for drug delivery systems.[2–7] Ongoing research continues to expand the scope of applications for CNTs, particularly in exploring colloidal properties, dispersion characteristics, heterogeneous electron transfer capabilities, and plasmon enhancement effects. These attributes leverage the unique combination of electrical conductivity, susceptibility to chemical modification, and biodegradability of CNTs, thereby enhancing their potential in advancing cutting-edge biomedical technologies.[8–12]

A notable challenge with pristine CNTs is their inert surface and poor dispersion in solvents, necessitating the selection of appropriate organic solvents like N-Methyl-2-pyrrolidone (NMP) and dimethylformamide (DMF) to disperse CNTs efficiently.[13] However, organic solvents are unsuitable for biological applications as they disrupt the native structure of enzymes and can denature sensitive proteins and aptamers due to their toxic effects, compromising their biological activity and downstream biological assays. To enhance the solubility and dispersion of CNTs, researchers have devised various methods such as surface modification, surface functionalization using hydrophilic materials and polymers, and decorating CNTs with organometallic nanoparticles.[7,14] Incorporating metal nanoparticles significantly enhances the inherent characteristics of CNTs, making them ideal for specific applications in gas sensors, toxicant sensors, and catalysis, where they play a critical role in signal amplification and sensitivity.[15–22] Gold nanoparticles (AuNPs) are exceptionally suitable for biological applications due to their biocompatibility, catalytic activity, and surface plasmon resonance.[23–26] Decorating CNTs with AuNPs offers several advantages, as the resulting nanohybrids exhibit a synergistic effect, enhancing conductivity, creating extensive networks, and ensuring biocompatibility while reducing cytotoxicity.[27,28] These nanohybrids can be accomplished through several approaches such as physical or wet chemical deposition, where gold nanoparticles are either adsorbed onto the CNT surface or covalently attached.[29,30] However, physical adsorption has lower stability and relies on a tedious, multistep, layer-by-layer deposition process.[31–33] On the other hand, the direct deposition method using wet chemical processes has been employed to attach gold nanoparticles to the surface of CNTs covalently.[34] Nevertheless, this approach poses three major challenges: 1) the use of toxic chemicals for modification, 2)

View Article Online
DOI: 10.1039/D5TB00990A

inconsistent and diverse particle size decoration, and 3) gold nanoparticle aggregation which obstructs the electroactive surface area (EASA) and hinders the electrochemical performance of the nanohybrid. Achieving uniform and controlled gold deposition on CNT surfaces while maintaining simplicity and ease of use has proven to be difficult.[35] Various interlinkers have been employed to address these issues, generating stable nanohybrids through electrostatic and covalent interactions between AuNPs and CNTs.[36,37] This strategy holds promise as it enables control over nanoparticle size, ensures secure bonding, and minimizes adverse environmental effects by eliminating toxic chemicals such as thionyl chloride for surface modification.

In this study, we propose a facile, chemically stable, and controlled synthesis approach for uniformly decorating gold nanoparticles over CNT surfaces at room temperature. Our method involves utilizing hetero-functional polyethylene glycol (PEG) as a linker between AuNPs and CNTs, forming a stable covalent bond through EDC/NHS chemistry. By introducing PEG directly into the AuNP solution, we modify the AuNP surface to enhance stability and prevent aggregation during the decoration process on the CNT surface. This technique guarantees that the resulting Au-CNTs demonstrate a uniform distribution of AuNPs with consistent particle sizes, leading to improved dispersion, enhanced electron transfer, and an ideal surface for immobilizing aptamers and proteins. This Au-CNT nanohybrid exhibits improved dispersion and can be seamlessly incorporated into protein or biopolymer matrices, maintaining extended channels for conductivity. Crucially, our synthesis method ensures that the Au-CNTs remain environmentally safe and biodegradable, minimizing their impact on the environment. For proof-of-concept feasibility studies, H_2O_2 and glucose sensor were developed using an Au-CNT nanohybrid with electrodeposited Prussian Blue as a redox mediator. This approach demonstrates superior performance compared to CNT alone. The biocompatible Au-CNT nanohybrid exhibits rapid kinetics, a larger surface area, and enhanced electrochemical properties, making it an ideal multifunctional nanomaterial for affinity and catalytic biosensors.

2. Materials and Methods

2.1 Materials

Heterobifunctional polyethylene glycol (HS-PEG-NH_2), hydrochloric acid (HCl), Multiwalled Carbon Nanotubes (MWCNTs avg. dia. × L: 9.5 nm × 1.5 μm), sodium hydroxide (NaOH, >97%), hydrogen tetrachloroaurate(III) trihydrate ($HAuCl_4 \cdot 3H_2O$, ≥99%), 2-(N-morpholino) ethane sulfonic acid buffer (MES hydrate,≥99%), sulfuric acid (H_2SO_4), Iron(III) chloride ($FeCl_3$), Potassium chloride (KCl), Sodium citrate dihydrate ($Na_3C_6H_5O_7.2H_2O$≥99.9%), potassium hexacyanoferrate(II) trihydrate ($K_4Fe(CN)_6 \cdot 3H_2O$, 98.5%–99%), potassium hexacyanoferrate(III) ($K_3Fe(CN)_6$,

≥99.0%), Sodium chloride (NaCl), N-hydroxy succinimide (NHS, $C_4H_5NO_3$, ≥98%), N-ethyl-N'-(3-dimethylaminopropyl) carbodiimide hydrochloride (EDC, $C_8H_{17}N_3 \cdot HCl$, ≥99.0%), Bovine serum albumin (BSA), Glucose Oxidase, Glutaraldehyde (GA 25%), Uric acid (UA), Hydrogen peroxide (H_2O_2 30% w/v), L-Ascorbic acid (AA) and dextrose (D-glucose) were bought from Sigma-Aldrich. SPCE electrodes were purchased from Zensor R&D Co. Unless otherwise stated, all solutions were prepared via deionized water (DI) exhibiting resistivity of 18.2 MΩ.

2.2 Instrumentation

Different microscopic techniques were used to analyze the morphological and physio-chemical structure of Au-CNT nanohybrid. Field Emission scanning electron microscope (FESEM, JEOL JSM-6330) was used to investigate the surface structure and properties. To verify the uniform decoration of (AuNPs) on the surface of (MWCNTs), Field Emission Gun Transmission Electron Microscope (FEG -TEM, Tecnai G2 F30 S-TWIN) was employed. This approach allowed us to perform detailed line profile analysis and mapping of the synthesized Au-CNT nanohybrid. In addition, we performed a chemical analysis of Au-CNT using Fourier transform infrared spectroscopy (ATR-FTIR, Thermos Scientific Nicolet iS5). To examine the crystal structure and chemical composition of Au-CNT nanohybrid high-resolution photoelectric spectroscopy (XPS, JEOL JPS 9030) and Powder X-Ray diffractometer (Bruker D2-Phaser) were employed. UV-Vis spectroscopy is utilized to precisely monitor the PEGylated AuNPs stability and decoration over the CNT surface using UV- Vis spectrophotometer (Flexa A-200 HT). For our electrochemical studies, (Autolab PGSTAT204) electrochemical workstation was used. The electrochemical characterization was conducted using a screen-printed carbon electrode (SPCE) which comprised of three-electrode system. This system included a counter electrode, a working electrode and a reference electrode made of Ag/AgCl paste.

2.3 Synthesis Method

Figure 1 illustrates the two-step process of decorating MWCNTs with PEGylated gold nanoparticles, including functionalization and covalent bond formation.

1) Synthesis of PEG-AuNPs: AuNPs were synthesized employing a well-documented method involving the reduction of $HAuCl_4$ with sodium citrate.[38] In this experiment, approximately 0.05 g of $HAuCl_4$ was dissolved in 150 ml of deionized (DI) water and heated to 300°C. Subsequently, about 0.132 g of sodium citrate dissolved in 15 ml of DI water was added to the heated solution and stirred for 2 hours to produce gold nanoparticles, which exhibited a distinct ruby-red colour. After cooling the gold nanoparticle solution to room temperature, 0.15 g of heterobifunctional polyethylene

View Article Online
DOI: 10.1039/D5TB00990A

glycol (PEG) was dissolved in approximately 37.5 ml of the gold citrate solution. The resulting gold nanoparticle and PEG solution were then stored at 4°C for subsequent use.

2) Oxidation of MWCNT and gold nanoparticle decoration: The MWCNTs were chemically oxidized using a 3:1 mixture of HCl and H_2SO_4 to introduce carboxylic groups. After modification, the MWCNT solution underwent multiple rounds of centrifugation and washing, followed by vacuum drying. Subsequently, 1 mg of MWCNTs was subjected to EDC/NHS in a 2:1 ratio prepared in MES buffer and sonicated for 30 minutes. Post-sonication, the MWCNT solution was centrifuged to remove excess reagents. Finally, 5 ml of PEG-AuNPs solution was added to 5 mg of oxidized MWCNTs to synthesize the Au-CNT nanohybrid.

2.4 Electrode surface modification and electrochemical measurements

The working electrode of screen-printed carbon electrodes (SPCEs)is modified by drop-casting approximately 8 µL of a 1 mg/mL solution of carbon nanotubes (CNTs) and gold-carbon nanotube (Au-CNT) nanohybrids, which were prepared in deionized water. After modification, the electrodes were dried using an incubator at 37°C for 6 hours before performing any electrochemical analysis.

Cyclic voltammetry (CV) was used to investigate the electrochemical charge transfer behaviour and its dependence on scan rate. By analysing the voltammograms recorded at various scan rates, the electrochemical performance of the different modified electrodes, SPCE/CNT and SPCE/Au-CNT were compared. These voltammograms revealed key insights into the redox properties and electron transfer dynamics of the modified electrodes. It was clear that the incorporation of gold nanoparticles over the CNT surface improved electron transfer and redox behaviour compared to the CNT alone. To showcase the practical potential of the Au-CNT nanohybrid, glucose and H_2O_2 sensor were developed to demonstrate its applicability. Both sensors utilize Prussian Blue (PB) as a common redox mediator to compare their catalytic performance.

2.5 Development of catalytic biosensor

To fabricate a Prussian Blue (PB)-based sensor, the working electrode of SPCE is rinsed with (DI) water and then PB is electrodeposited via CV within a potential (range of -0.2 V - 0.5 V) vs. Ag/AgCl for 20 cycles. The deposition is performed using a freshly prepared PB solution containing 3 mM potassium ferricyanide ($K_3Fe(CN)_6$) and 3 mM ferric chloride ($FeCl_3$) dissolved in a 0.1 M solution of KCl and HCl. Following electrodeposition, the PB layer is stabilized and activated by additional CV cycling (20 cycles) in an equimolar solution containing KCl and HCl (0.1M). The modified electrode is then dried at 60°C for 1 hour.

To develop a hydrogen peroxide (H_2O_2) sensor, a thin layer of carbon nanotubes (CNT) or gold-carbon nanotube (Au-CNT) nanohybrid is drop-cast onto the PB-modified SPCE and allowed to dry. The superior catalytic performance of the Au-CNT nanohybrid compared to CNT alone highlights its potential for catalytic biosensor applications. Building on this performance, a glucose sensor is fabricated. Glucose enzyme solution is made by adding 5 mg of glucose oxidase (GOx) in 1 mL of phosphate-buffered saline. This solution is then mixed with an enzyme stabilizer including 1 mg of BSA and 0.8% GA. The resulting 7µl of enzyme mixture is immobilized onto SPCE/PB/CNT and SPCE/PB/Au-CNT modified electrodes and dried at 4°C. The catalytic performance and fabricated biosensor response to analyte concentration were analysed and compared using chronoamperometry using 0.1 M PBS solution under stirring conditions.

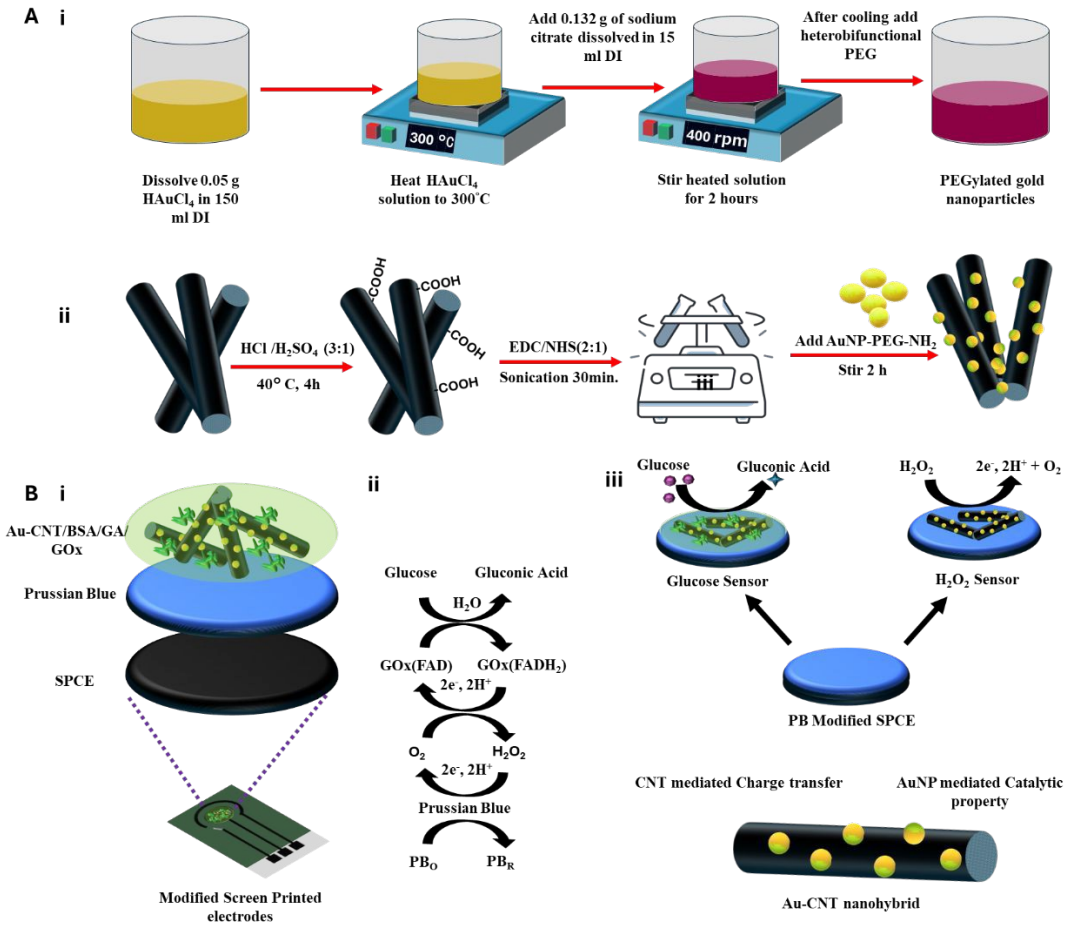

Figure 1: A) Schematic illustrating the step-by-step process for i) synthesizing PEGylated gold nanoparticles. ii) synthesizing Au-CNT nanohybrid using PEGylated gold nanoparticles. B) Schematic showing i) design, and components ii) possible

glucose mechanism and iii) properties of biocompatible Au-CNT and feasibility for catalytic biosensors.

3 Results and Discussion

3.1 Morphology and Surface Topography Characterization

The nanohybrid is engineered by decorating gold nanoparticles using a simple and effective strategy while keeping uniform particle size distribution over the MWCNT nanostructure. The morphological and nanostructural properties were examined with SEM. As represented in **Fig. 2(a)** oxidized MWCNTs have a rough texture, likely attributed to the chemical oxidation with HCl and H_2SO_4. The chemical oxidation of MWCNTs nanostructure is vital for the conjugation of PEGylated AuNPs. This modification allows the facile and controlled decoration of PEGylated gold nanoparticles owning similar particle size and morphology as depicted in **Fig.2(b)**. To further investigate the nanostructure morphology of Au-CNT nanohybrid HR-TEM was used. TEM images revealed that Au-CNT strands exhibit consistent morphology, with gold nanoparticles evenly decorated over the MWCNTs surface as demonstrated in **Fig. 2(c)**. We also analysed the morphology and particle size of PEGylated AuNPs as shown in **Fig. 2(d)**. Additionally, High-angle Annular Dark Field scanning electron microscopy was employed to investigate structural and elemental composition for both PEGylated AuNPs and Au-CNT nanohybrid as shown in **Fig. 2(e-i)**. Deeper structural insights were obtained from (HRTEM) images of the Au-CNT nanohybrid. **Fig. 2(j-l)** revealed well-defined lattice fringes in **Fig. 2(k)** and d- spacing of 2.1 Å in **Fig. 2(l)** corresponding to the typical (200) plane of Au nanoparticle.[39]

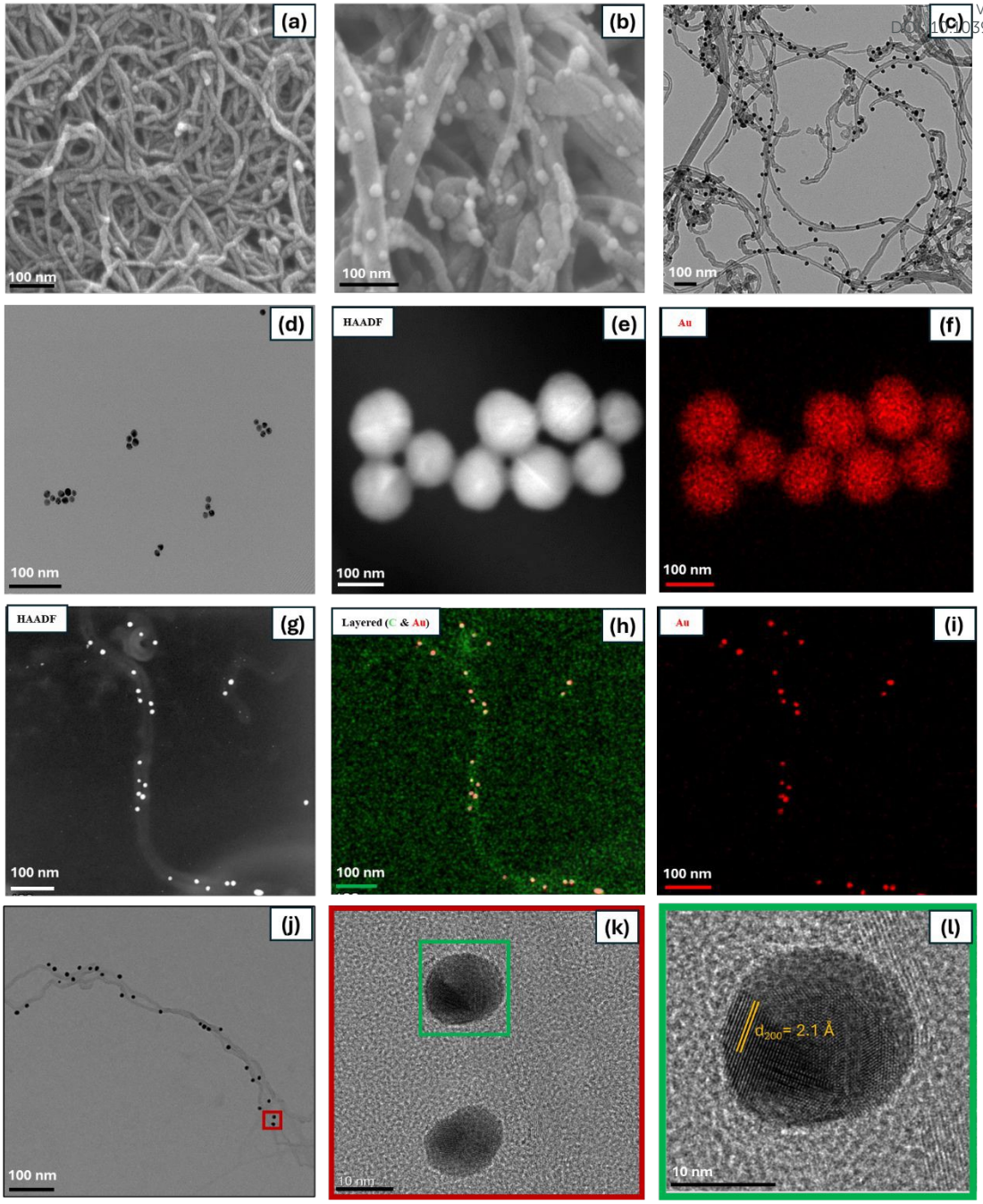

Figure 2: SEM images of (a) Oxidized MWCNT and (ii) Au-CNT nanohybrid. TEM image of (c) of Au-CNT nanohybrid and (d) PEGylated AuNPs. HAADF image of (e) PEGylated AuNPs, (f) EDS elemental map showing Au, HAADF image of (g) Au-CNT nanohybrid, EDS elemental map (h) showing a layered map of Au-CNT nanohybrid, (i) showing presence of Au. HRTEM images of (j) Au-CNT nanohybrid showing d-spacing in (k) (red) and (l) (green) corresponds to the (200) plane of gold nanoparticle with d spacing of 2.1 Å.

3.2 Chemical Composition Structural Characterization

ATR-FTIR spectroscopy was employed to investigate surface functionalities of nanostructures and synthesized Au-CNT nanohybrid as shown in **Fig. 3(a)**. All

nanomaterials were drop-casted onto SPCE electrodes before FTIR measurements, revealing a peak at 2347 cm^{-1}, which is attributed to (C=C) stretching. Oxidized MWCNTs exhibit characteristic peaks at 1079 cm^{-1}, 1712 $cm^{-1}$and a broad peak at 3328 cm^{-1} corresponding to (C-O), (C=O), and (O-H) stretching and bending modes respectively indicating the existence of COOH groups on MWCNT surface due to chemical oxidization by acid treatment.[40] AuNPs are functionalized with PEG coating on the surface as the PEGylated AuNPs exhibited peaks at 1048 cm^{-1}, 2598 cm^{-1} and 1569 cm^{-1}, 2858 cm^{-1}, and 3400 cm^{-1} which corresponds to (S=O), (S-H), (C-H) and (N-H) stretching vibrations respectively.[41] We further performed a salt test to validate the functionality and stability of PEGylated AuNPs in **Supplementary Fig. 1(b)**. After covalently attaching PEGylated AuNPs to the MWCNT surface via EDC/NHS chemistry, a significant reduction in peak intensities was observed. This reduction is attributed to the involvement of COOH and amine groups in forming amide bonds between the PEGylated AuNPs and the MWCNT nanostructures. Au-CNT nanohybrid shows additional peaks at 1530 cm^{-1}, and 1694 cm^{-1} which is attributed to (N-H) and (C=O) stretching from the resulting amide bond.[42] To further validate the surface elemental composition and chemical state of the Au-CNT nanohybrid XPS measurements were conducted as shown in **Fig. 3(b)**. The High-resolution XPS spectra of Au-CNT The nanohybrid exhibited distinct peaks associated with binding energies of C1s (286 eV), O1s (534eV), N1s (400 eV), and Au 4f (84, 88 eV).[43] These peaks were further deconvoluted to get deeper insights about phase constitution and electronic state Fig. **3(c-f)**. C1s spectrum has three subpeaks corresponding to (C-C), (C-N), and (C-O) representing the presence of PEGylated AuNPs over the MWCNT surface. The O1s spectrum revealed sharp subpeaks corresponding to (C=O) and (C-O), confirming the formation of amide bonds. Additionally, deconvoluted N1s and Au4f spectra further validate the successful covalent interaction between nanostructures. Au-CNT nanohybrid is expected to have better structural integrity and stability owning uniform decoration of gold nanoparticles with stable covalent bonding. To validate this hypothesis, XRD analysis was performed to examine the crystalline structure of Au-CNT nanohybrid as illustrated in **Fig. 3(g)**. XRD analysis revealed four different peaks at 26°, 37.8°, 44° and 64.4°. Notably, the sharp peak at 26° attributed to the (002) plane of interlayer spacing of graphitic carbon in Au-CNT nanohybrid.[44] Additional three prominent peaks at 37.8°,44°, and 64.4° compliant to (111), (200), and (220) lattice planes of AuNPs indicate high crystallinity and are consistent with XPS, HRTEM measurements.[45]

Raman spectroscopy acts as an extremely sensitive complementary tool for investigating the phase and electronic structure of Au-CNT nanohybrid. **Fig.3(h)** provides and comparative analysis between oxidised CNT and Au-CNT nanohybrid.

The Raman spectra revealed characteristic peaks at 1580 cm^{-1} (G-band) and 1350 cm^{-1} (D-band) both before and after the decoration of AuNPs on the CNT surface. The prominent G-band implies the presence of sp^2-hybridized carbon atoms in a graphitic structure, while the D-band indicates the presence of defects and disorder. The higher ID/IG ratio of the CNTs before decoration indicates a high level of defects due to chemical oxidation.[46] However, this ratio decreases after the covalent interaction with AuNPs, suggesting a reduction in defects.[47] **Fig. 3(i)** shows the comparative adsorption spectra between PEGylated AuNPs, CNT, and Au-CNT nanohybrid. The UV-Vis spectra revealed a typical absorption peak at 525 nm for PEGylated AuNPs, attributed to Surface Plasmon Resonance.[48] In contrast, CNTs do not show distinct absorption peaks but exhibit a flat absorption profile with higher intensity. However, after decorating the CNTs with AuNPs, a slight red shift in the absorption peak was observed, indicating changes in the electronic structure and covalent interactions between the AuNPs and CNTs. All physiochemical characterization on Au-CNT nanohybrid validates and supports the covalent functionalization of PEGylated AuNPs over the CNT surface. The Au-CNT nanohybrid exhibits a similar morphology with a uniform decoration of gold nanoparticles across the surface. This nanohybrid is expected to have improved dispersion, solubility, conductivity, and superior electrochemical performance compared to pristine CNTs. Additionally, the Au-CNT nanohybrid offers an excellent surface for the immobilization of bio-recognition elements, making it highly suitable for electrochemical affinity biosensing applications.

View Article Online
DOI: 10.1039/D5TB00990A

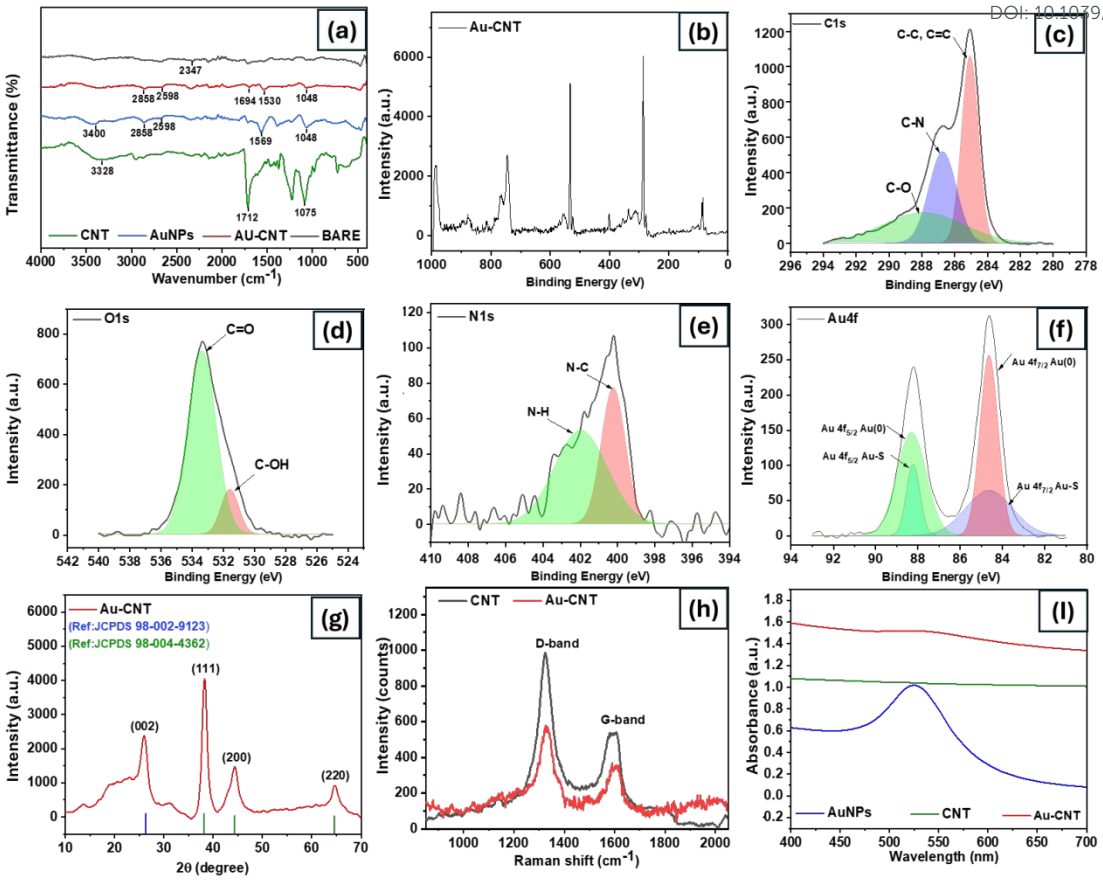

Figure 3: (a) FTIR spectra of oxidized MWCNT, AuNP-PEG, AU-CNT nanohybrid, and Bare SPCE. (b) High-resolution XPS spectra of synthesized Au-CNT nanohybrid. (c), (d), (e), (f) deconvoluted C1, O1, N1s, and Au respectively for Au-CNT nanohybrid. (g) XRD spectra for Au-CNT (h) Raman spectra of oxidized MWCNT and Au-CNT. (i) UV-visible spectrum of PEGylated AuNPs, CNT and Au-CNT nanohybrid.

3.3 Electrochemical Characterization electrode and coating

In our research, further electrochemical testing was conducted to thoroughly evaluate and compare the electrochemical properties of CNT and the synthesized Au-CNT nanohybrid. We applied a thin coating of CNT and Au-CNT nanohybrid over SPCE and utilized CV and Electrochemical Impedance Spectroscopy to gain a comprehensive understanding of the redox behaviour, electron transfer kinetics, and impedance characteristics of the Au-CNT nanohybrid. The EIS analysis revealed a higher charge transfer resistance (Rct) for the bare SPCE, attributed to lower conductivity and surface area, while both the modified SPCE/CNT and SPCE/Au-CNT exhibited a linear profile at the lower frequency range, as indicated by the Nyquist plot in **Fig. 4(a)**, suggesting improved mass transport and faster electron transfer kinetics. The CV curves showed SPCE/Au-CNT electrode depicts higher peak current and lower peak separation than SPCE/CNT and bare SPCE, indicating faster electron transfer kinetics as shown in **Fig. 4(b)**. The SPCE/Au-CNTs electrode exhibits better charge transfer and is expected to

have higher electrochemical active surface area than SPCE/CNT. To further investigate this, we performed CV using 5 mM solution of $[Fe(CN)_6]^{2-}/[Fe(CN)_6]^{3-}$ at different scan rates, (ranging from 0.02 to 0.1 V/s), and the subsequent voltammograms are shown in **Fig. 4 (c, d, e)**. As the scan rate increased, there was a linear rise in the peak current values. This relationship is evident from the linear fit of both Oxidation and reduction peak currents plotted as a function of the square root of the scan rate, as illustrated in **Fig. 4(f)**, indicating that Au-CNT exhibit excellent electrochemical performance compared to pristine CNTs. Moreover, the EIS data was fitted to an appropriate equivalent circuit model built on the Randles circuit, as illustrated in **Supplementary Fig. 2(b)**, which aligns with the impedance data represented in **Supplementary Fig. 3(a, b, c)**. The Au-CNT nanohybrids feature uniformly distributed AuNPs covalently bonded to the CNT surface, significantly increasing the electroactive surface area as illustrated in **Supplementary table 2.** This enhancement facilitates rapid electron transport, making Au-CNT nanohybrid ideal for applications in electrochemical biosensing and energy storage devices.

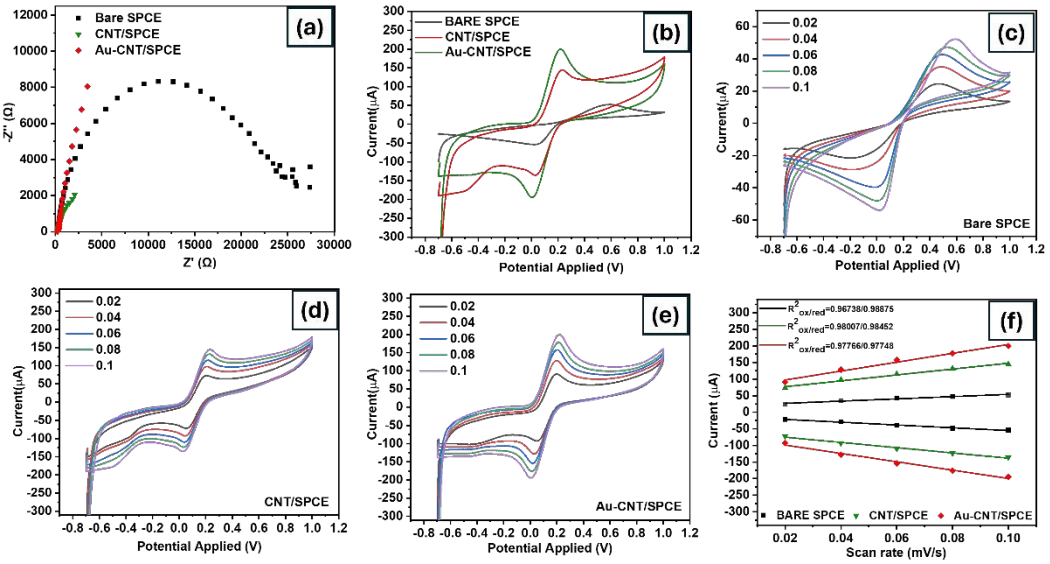

Figure 4: (a) Nyquist plots observed during EIS investigations, (b) circular voltammograms depicting electrochemical performance of SPCE, modified SPCE/CNT and SPCE/Au-CNT in 5 mM solution of $[Fe(CN)_6]^{2-}/[Fe(CN)_6]^{3-}$. CV of the (c) SPCE, modified (d) SPCE/CNT and (e) SPCE/Au-CNT at various scan rates and (f) presenting the extracted oxidation and reduction peak current values from bare SPCE, CNT/SPCE, SPCE/Au-CNT compared and plotted against square root of the scan rate.

3.4 Catalytic performance and biosensor feasibility

Based on electrochemical performance, it is anticipated that the Au-CNT nanohybrid

will exhibit superior catalytic activity due to the presence of AuNPs on its surface, which significantly enhances its electrocatalytic surface area. To investigate this hypothesis, we compared the catalytic performance of the modified electrodes, SPCE/PB/CNT and SPCE/PB/Au-CNT, with electrodeposited Prussian as a redox mediator. The electrodeposition process was carried out using multiple cycles of CV, as illustrated in **Fig. 5(a)**. The electrochemical performance of SPCE/PB/CNT and SPCE/PB/Au-CNT was assessed through H_2O_2 sensing using chronoamperometry at -0.4 V in a stirred 0.1 M PBS solution spiked with 0.5 mM H_2O_2, optimizing the performance and sensitivity of the modified electrodes. The real-time chronoamperometry current responses of the Au-CNT nanohybrid modified electrode to H_2O_2 showed significant improvements, demonstrating that the Au-CNT nanohybrid exhibits enhanced catalytic performance. This makes it a promising candidate for developing electroenzymatic sensors, as evident from **Fig. 5(b)**. To further investigate this, a proof-of-concept glucose sensor was developed using the same sensing mechanism, with PB acting as the redox mediator.[49] The entire sensor fabrication process was monitored, and each step was characterized by CV, as shown in **Supplementary Fig. 5(a)**. To account for any variations in electrode performance after PB deposition, the different modified PB/SPCE electrodes were compared using CV in a 0.1 M KCl solution, as shown in **Supplementary Fig. 5(b)**. The modified electrodes, SPCE/PB/CNT and SPCE/PB/Au-CNT, were then functionalized with a glucose oxidase enzyme layer, and the morphology of the modified electrodes was examined using SEM, as shown in **Supplementary Fig. 6**. Real-time current responses of the modified electrodes to glucose were recorded using chronoamperometry at 0.6 V in a stirred 0.1 M PBS solution, spiked with 0.5 mM glucose as shown in **Fig. 5(d).**

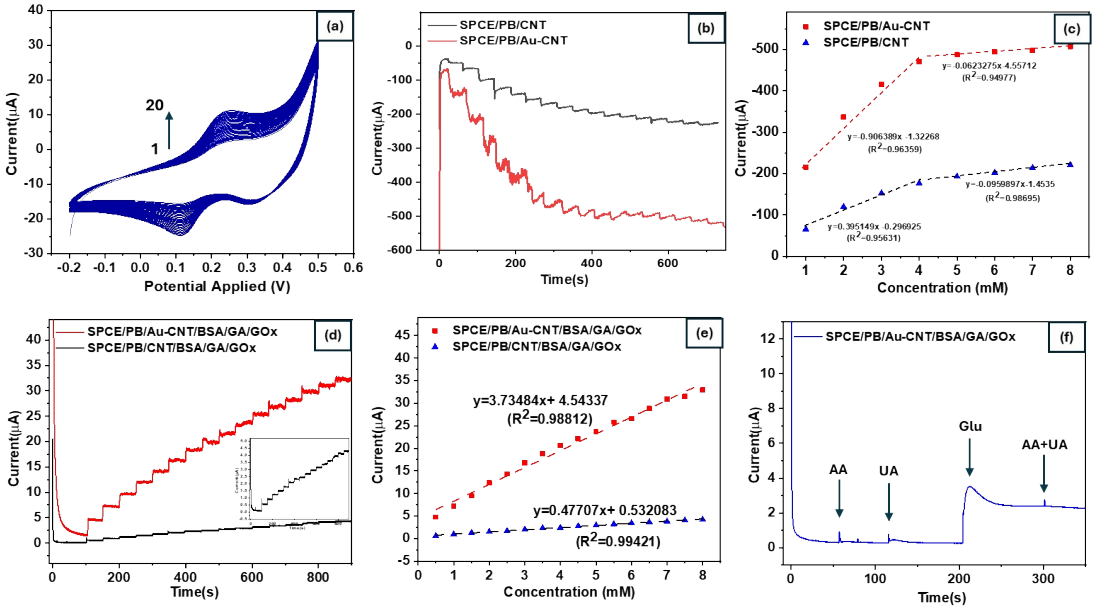

Figure 5: Electrodeposition of Prussian Blue on (SPCE) and sensor performance for

H_2O_2 and glucose detection. (a) CV showing the deposition cycles of PB on SPCE. (b) H_2O_2 sensing performance using Au-CNT and CNT drop-cast on PB-modified SPCE at a potential of -0.4 V. (c) Sensor response upon the addition of H_2O_2 to the PB-modified SPCE. (d) Glucose sensing performance with different conductive fillers at 0.6 V (each step representing electrode response after spiking with 0.5 mM of glucose solution). (e) Extracted step peak current versus glucose concentration. (f) interference test adding equimolar (0.5mM) of ascorbic acid, uric acid, glucose and uric acid + ascorbic acid under stirring condition in 0.1 M PBS.

This refined analysis highlights the enhanced catalytic performance of the Au-CNT nanohybrid, attributed to its improved electron transfer efficiency and increased surface area. As represented in **Fig. 5(d)**, the performance of the developed biosensor was additionally assessed using the amperometric i-t response. Upon the addition of glucose, both the SPCE/PB/Au-CNT/BSA/GA/GOx and SPCE/PB/CNT/BSA/GA/GOx modified electrodes exhibited a rapid increase in response current, reaching 95% of their steady-state value within just 2 seconds. This demonstrates the fast response time of the modified electrodes to glucose. The linear concentration ranges for both electrodes spanned from 0.5 to 8.00 mM, which is within the clinically relevant range for glucose detection. The SPCE/PB/Au-CNT/BSA/GA/GOx electrode exhibited a limit of detection (LOD) of 31.2 µM and a sensitivity of 53.35 $\mu A \cdot mM^{-1} \cdot cm^{-2}$, while the SPCE/PB/CNT/BSA/GA/GOx electrode displayed a sensitivity of 6.815 $\mu A \cdot mM^{-1} \cdot cm^{-2}$ and an LOD of 246 µM. The SPCE/PB/Au-CNT/BSA/GA/GOx electrode demonstrated nearly 8 times higher sensitivity towards glucose compared to the CNT-modified electrode. This enhanced sensitivity can be attributed to the Au-CNT nanohybrid, which is decorated with AuNPs to enable rapid kinetics, while the CNT provides extensive conductive channels for efficient charge transfer. The AuNPs play a crucial role in improving charge transfer, thereby enhancing the efficiency of glucose oxidation catalyzed by glucose oxidase.[50] To evaluate the selectivity of the SPCE/PB/Au-CNT/BSA/GA/GOx interface, a stirred 0.1 M PBS solution was spiked with an equal concentrations of common interfering species like Uric Acid and Ascorbic Acid, as illustrated in **Fig. 5(f)**. The real-time current response to common interferents was minimal compared to the response to glucose, which can be attributed to the selective enzyme layer composed of BSA/GA and GOx. This biorecognition interface not only enables specific catalytic detection of glucose but also acts as a physical and chemical barrier, minimizing the access of interfering species to the underlying PB layer. As a result, non-specific electrode responses are significantly reduced, enhancing the overall selectivity of the biosensor. These findings highlight the potential of the Au-CNT nanohybrid as a highly sensitive and effective material for the development of advanced biosensors. Its unique properties make it a promising

candidate for applications in biosensing and analytical chemistry, particularly in biomarker detection and real-time monitoring of biological processes.

Conclusion

In conclusion, we have developed a facile method for synthesizing a multifunctional Au-CNT nanohybrid, enabling controlled and uniform decoration of gold nanoparticles on the CNT surface. This nanohybrid exhibits enhanced electrochemical properties, superior electron transfer kinetics, and robust potential for bioconjugation with a variety of recognition elements such as enzymes, aptamers, antibodies, and proteins. To demonstrate its practical utility, a glucose oxidase based electrochemical biosensor was fabricated using the Au-CNT nanohybrid. The resulting sensor (SPCE/PB/Au-CNT/BSA/GA/GOx) showed a significantly improved performance, with a sensitivity of 53.35 μA mM^{-1} cm^{-2} and a LOD of 31.2 μM. In comparison, the CNT-only sensor (SPCE/PB/CNT/BSA/GA/GOx) exhibited a lower sensitivity of 6.815 μA mM^{-1} cm^{-2} and a higher LOD of 246 μM, both measured over the same linear detection range of 0.5–8.0 mM. These findings clearly highlight the superior performance of the Au-CNT nanohybrid in electrochemical biosensing applications. Owing to its excellent biocompatibility, high surface area, and ability to form a well-dispersed and conductive nanostructured network, the Au-CNT hybrid offers promising potential for a broad range of electrochemical catalytic and affinity biosensors, particularly for clinically important analytes.

Authorship contribution statement

Aditya Manu Bharti: Conceptualization, Investigation, data collection**,** writing original draft; **Terry Ting-Yu Chiou**: resources; **R. K. Rakesh Kumar**: Visualization, Analysis of experimental results; **Muhammad Omar Shaikh**: validation, Writing – review & editing; **Cheng-Hsin Chuang**: Supervision, Funding acquisition, Project administration.

Conflict of interest

There are no conflicts to declare.

Data availability statement

The data supporting this article have been included as part of the Supplementary Information.

Acknowledgements

View Article Online
DOI: 10.1039/D5TB00990A

The authors would like to thank the Ministry of Science and Technology, Taiwan, for financially supporting this research under Contract No. NSTC 113-2221-E-110 -034 - MY2.

Author's contribution

[#]Aditya Manu Bharti and Terry Ting-Yu Chiou have equally contributed to this work.

References

(1) Popov, Valentin N. "Carbon nanotubes: properties and application." *Materials Science and Engineering: R: Reports* 43, no. 3 (2004): 61-102.

(2) Rohrbach, Falk, Hakan Karadeniz, Arzum Erdem, Michael Famulok, and Günter Mayer. "Label-free impedimetric aptasensor for lysozyme detection based on carbon nanotube-modified screen-printed electrodes." *Analytical biochemistry* 421, no. 2 (2012): 454-459.

(3) Manoj, Devaraj, Rajendran Saravanan, Atchudan Raji, and Arumugam Thangamani. "Carbon-based microelectrodes for environmental remediation: progress, challenges and opportunities." *Carbon Letters* 33, no. 6 (2023): 1485-1493.

(4) Muqaddas, Sheza, Mohsin Javed, Sohail Nadeem, Muhammad Adeel Asghar, Ali Haider, Muhammad Ahmad, Ahmad Raza Ashraf et al. "Carbon nanotube fiber-based flexible microelectrode for electrochemical glucose sensors." *ACS omega* 8, no. 2 (2023): 2272-2280.

(5) Sun, Yafen, Nan Zhang, Qinrong Sun, Xiaoling Cao, Xuefeng Shao, and Yanping Yuan. "A novel form-stable phase change material based on elastomeric copolymer and carbon nanotubes with photo-thermal conversion performance." *Journal of Energy Storage* 63 (2023): 107043.

(6) Zhu, Jiayi, Liu Huang, Feng Bao, Guanli Chen, Kangjin Song, Zheling Wang, Hong Xia et al. "Carbon materials for enhanced photothermal conversion: Preparation and applications on steam generation." *Materials Reports: Energy* 4, no. 2 (2024): 100245.

(7) Shaikh, Muhammad Omar, Pei-Yu Zhu, Cheng-Chien Wang, Yi-Chun Du, and Cheng-Hsin Chuang. "Electrochemical immunosensor utilizing electrodeposited Au nanocrystals and dielectrophoretically trapped PS/Ag/ab-HSA nanoprobes for detection of microalbuminuria at point of care." *Biosensors and Bioelectronics* 126 (2019): 572-580.

(8) Zhang, Dengsong, Liyi Shi, Jianhui Fang, Xuanke Li, and Kai Dai. "Preparation and modification of carbon nanotubes." *Materials Letters* 59, no. 29-30 (2005): 4044-4047.

(9) Kim, Jin Ah, Dong Gi Seong, Tae Jin Kang, and Jae Ryoun Youn. "Effects of surface modification on rheological and mechanical properties of CNT/epoxy composites." *Carbon* 44, no. 10 (2006): 1898-1905.

(10) Wang, Bin, Yang Hu, Bo Yu, Xiaojuan Zhang, Dongxu Yang, and Yuanfu Chen. "Heterogeneous CoFe–Co8FeS8 nanoparticles embedded in CNT networks as highly efficient and stable electrocatalysts for oxygen evolution reaction." *Journal of Power Sources* 433 (2019): 126688.

(11) Jiang, Linqin, Lian Gao, and Jing Sun. "Production of aqueous colloidal dispersions of carbon nanotubes." *Journal of colloid and interface science* 260.1 (2003): 89-94.

(12) Wu, Yizeng, Xuewei Zhao, Yuanyuan Shang, Shulong Chang, Linxiu Dai, and Anyuan Cao. "Application-driven carbon nanotube functional materials." *ACS nano* 15, no. 5 (2021): 7946-7974.

(13) Kim, Ki Kang, S-M. Yoon, J-Y. Choi, Jeonghee Lee, B-K. Kim, Jong Min Kim, J-H. Lee et al. "Design of dispersants for the dispersion of carbon nanotubes in an organic solvent." *Advanced Functional Materials* 17, no. 11 (2007): 1775-1783.

(14) Kim, Sang Won, Taehoon Kim, Yern Seung Kim, Hong Soo Choi, Hyeong Jun Lim, Seung Jae Yang, and Chong Rae Park. "Surface modifications for the effective dispersion of carbon nanotubes in solvents and polymers." *Carbon* 50, no. 1 (2012): 3-33.

(15) Rana, Md Masud, Dauda Sh Ibrahim, M. R. Mohd Asyraf, S. Jarin, and Amanullah Tomal. "A review on recent advances of CNTs as gas sensors." *Sensor Review* 37, no. 2 (2017): 127-136.

(16) Septiani, Ni Luh Wulan, and Brian Yuliarto. "The development of gas sensor based on carbon nanotubes." *Journal of The Electrochemical Society* 163.3 (2016): B97.

(17) Zhang, Ting, Syed Mubeen, Nosang V. Myung, and Marc A. Deshusses. "Recent progress in carbon nanotube-based gas sensors." *Nanotechnology* 19, no. 33 (2008): 332001.

(18) Audevard, Jeremy, Anas Benyounes, Ruben Castro Contreras, Hicham Abou Oualid, Mohamed Kacimi, and Philippe Serp. "Multifunctional Catalytic Properties of Pd/CNT Catalysts for 4-Nitrophenol Reduction." *ChemCatChem* 14, no. 4 (2022): e202101783.

(19) Serp, Philippe, and Eva Castillejos. "Catalysis in carbon nanotubes." *ChemCatChem* 2.1 (2010): 41-47.

(20) Ahmed, Syed Rahin, Jeonghyo Kim, Tetsuro Suzuki, Jaebeom Lee, and Enoch Y. Park. "Enhanced catalytic activity of gold nanoparticle-carbon nanotube hybrids for influenza virus detection." *Biosensors and Bioelectronics* 85 (2016): 503-508.

(21) Gill, Sukhbir Singh, Tanish Goyal, Megha Goswami, Preeti Patel, Ghanshyam Das

Gupta, and Sant Kumar Verma. "Remediation of environmental toxicants using carbonaceous materials: opportunity and challenges." *Environmental Science and Pollution Research* 30, no. 27 (2023): 69727-69750.

(22) Pokhrel, Lok R., Nicholas Ettore, Zachary L. Jacobs, Asha Zarr, Mark H. Weir, Phillip R. Scheuerman, Sushil R. Kanel, and Brajesh Dubey. "Novel carbon nanotube (CNT)-based ultrasensitive sensors for trace mercury (II) detection in water: A review." *Science of the Total Environment* 574 (2017): 1379-1388.

(23) Falahati, Mojtaba, Farnoosh Attar, Majid Sharifi, Ali Akbar Saboury, Abbas Salihi, Falah Mohammad Aziz, Irena Kostova et al. "Gold nanomaterials as key suppliers in biological and chemical sensing, catalysis, and medicine." *Biochimica et Biophysica Acta (BBA)-General Subjects* 1864, no. 1 (2020): 129435.

(24) Bedford, Erin E., Jolanda Spadavecchia, Claire-Marie Pradier, and Frank X. Gu. "Surface plasmon resonance biosensors incorporating gold nanoparticles." *Macromolecular bioscience* 12, no. 6 (2012): 724-739.

(25) Liang, Aihui, Qingye Liu, Guiqing Wen, and Zhiliang Jiang. "The surface-plasmon-resonance effect of nanogold/silver and its analytical applications." *TrAC Trends in Analytical Chemistry* 37 (2012): 32-47.

(26) Sharma, Aditya, Zimple Matharu, G. Sumana, Pratima R. Solanki, C. G. Kim, and B. D. Malhotra. "Antibody immobilized cysteamine functionalized-gold nanoparticles for aflatoxin detection." *Thin Solid Films* 519, no. 3 (2010): 1213-1218.

(27) Singh, Rajpal, Thathan Premkumar, Ji-Young Shin, and Kurt E. Geckeler. "Carbon Nanotube and Gold-Based Materials: A Symbiosis." *Chemistry–A European Journal* 16, no. 6 (2010): 1728-1743.

(28) Alim, Samiul, Jaya Vejayan, Mashitah M. Yusoff, and A. K. M. Kafi. "Recent uses of carbon nanotubes & gold nanoparticles in electrochemistry with application in biosensing: A review." *Biosensors and Bioelectronics* 121 (2018): 125-136.

(29) Rakesh Kumar, R. K., Muhammad Omar Shaikh, Amit Kumar, Chi-Hao Liu, and Cheng-Hsin Chuang. "Zwitterion-functionalized cuprous oxide nanoparticles for highly specific and enzymeless electrochemical creatinine biosensing in human serum." *ACS Applied Nano Materials* 6, no. 3 (2023): 2083-2094.

(30) Wu, Bohua, Yinjie Kuang, Xiaohua Zhang, and Jinhua Chen. "Noble metal nanoparticles/carbon nanotubes nanohybrids: synthesis and applications." *Nano Today* 6, no. 1 (2011): 75-90.

(31) Cai, Xiaojun, Xia Gao, Lisha Wang, Qi Wu, and Xianfu Lin. "A layer-by-layer assembled and carbon nanotubes/gold nanoparticles-based bienzyme biosensor for cholesterol detection." *Sensors and Actuators B: Chemical* 181 (2013): 575-

View Article Online
DOI: 10.1039/D5TB00990A

583.

(32) Zhang, Meining, Lei Su, and Lanqun Mao. "Surfactant functionalization of carbon nanotubes (CNTs) for layer-by-layer assembling of CNT multi-layer films and fabrication of gold nanoparticle/CNT nanohybrid." *Carbon 44.2 (2006): 276-283.*

(33) Wang, Ying, Wanzhi Wei, Xiaoying Liu, and Xiandong Zeng. "Carbon nanotube/chitosan/gold nanoparticles-based glucose biosensor prepared by a layer-by-layer technique." *Materials Science and Engineering: C* 29, no. 1 (2009): 50-54.

(34) Lorençon, Eudes, Andre S. Ferlauto, Sergio de Oliveira, Douglas R. Miquita, Rodrigo R. Resende, Rodrigo G. Lacerda, and Luiz O. Ladeira. "Direct production of carbon nanotubes/metal nanoparticles hybrids from a redox reaction between metal ions and reduced carbon nanotubes." *ACS applied materials & interfaces* 1, no. 10 (2009): 2104-2106.

(35) Georgakilas, Vasilios, Dimitrios Gournis, Vasilios Tzitzios, Lucia Pasquato, Dirk M. Guldi, and Maurizio Prato. "Decorating carbon nanotubes with metal or semiconductor nanoparticles." *Journal of Materials Chemistry* 17, no. 26 (2007): 2679-2694.

(36) Li, Nan, Qiang Xu, Min Zhou, Wei Xia, Xingxing Chen, Michael Bron, Wolfgang Schuhmann, and Martin Muhler. "Ethylenediamine-anchored gold nanoparticles on multi-walled carbon nanotubes: Synthesis and characterization." *Electrochemistry communications* 12, no. 7 (2010): 939-943.

(37) Duc Chinh, Vu, Giorgio Speranza, Claudio Migliaresi, Nguyen Van Chuc, Vu Minh Tan, and Nguyen-Tri Phuong. "Synthesis of gold nanoparticles decorated with multiwalled carbon nanotubes (Au-MWCNTs) via cysteaminium chloride functionalization." *Scientific reports* 9, no. 1 (2019): 5667.

(38) Ji, Xiaohui, Xiangning Song, Jun Li, Yubai Bai, Wensheng Yang, and Xiaogang Peng. "Size control of gold nanocrystals in citrate reduction: the third role of citrate." *Journal of the American Chemical Society* 129, no. 45 (2007): 13939-13948.

(39) Torres-Mendieta, Rafael, David Ventura-Espinosa, Sara Sabater, Jesus Lancis, Gladys Mínguez-Vega, and Jose A. Mata. "In situ decoration of graphene sheets with gold nanoparticles synthetized by pulsed laser ablation in liquids." *Scientific reports* 6, no. 1 (2016): 30478.

(40) De Menezes, B. R. C., F. V. Ferreira, B. C. Silva, E. A. N. Simonetti, T. M. Bastos, L. S. Cividanes, and G. P. Thim. "Effects of octadecylamine functionalization of carbon nanotubes on dispersion, polarity, and mechanical properties of CNT/HDPE nanocomposites." *Journal of materials science* 53, no. 20 (2018): 14311-14327.

(41) Leopold, Loredana Florina, István Szabolcs Tódor, Zoriţa Diaconeasa, Dumitriţa Rugină, Andrei Ştefancu, Nicolae Leopold, and Cristina Coman. "Assessment of PEG and BSA-PEG gold nanoparticles cellular interaction." *Colloids and Surfaces A: Physicochemical and Engineering Aspects* 532 (2017): 70-76.

(42) Bharti, Aditya Manu, RK Rakesh Kumar, Cheng-Hsin Chuang, and Muhammad Omar Shaikh. "Universal nanocomposite coating with antifouling and redox capabilities for electrochemical affinity biosensing in complex biological fluids." *Nanoscale Horizons* 9, no. 5 (2024): 843-852.

(43) Ouyang, Ruizhuo, Penghui Cao, Pengpeng Jia, Hui Wang, Tianyu Zong, Chenyu Dai, Jie Yuan et al. "Bistratal Au@ Bi2S3 nanobones for excellent NIR-triggered/multimodal imaging-guided synergistic therapy for liver cancer." *Bioactive Materials* 6, no. 2 (2021): 386-403.

(44) Huq, Mohammad Mahmudul, Chien-Te Hsieh, and Chia-Yin Ho. "Preparation of carbon nanotube-activated carbon hybrid electrodes by electrophoretic deposition for supercapacitor applications." *Diamond and Related Materials 62 (2016): 58-64.*

(45) Krishnamurthy, Sneha, Andrea Esterle, Nilesh C. Sharma, and Shivendra V. Sahi. "Yucca-derived synthesis of gold nanomaterial and their catalytic potential." *Nanoscale research letters* 9 (2014): 1-9.

(46) Chen, Wei, Lujiang Huang, Jun Hu, Tengfei Li, Feifei Jia, and Yu-Fei Song. "Connecting carbon nanotubes to polyoxometalate clusters for engineering high-performance anode materials." *Physical Chemistry Chemical Physics* 16, no. 36 (2014): 19668-19673.

(47) Young, Sheng-Joue, and Zheng-Dong Lin. "Ethanol gas sensors composed of carbon nanotubes with Au nanoparticles adsorbed onto a flexible PI substrate." *ECS Journal of Solid State Science and Technology* 6, no. 10 (2017): M130.

(48) Hao, Liling, XuTao Liu, Sunjie Xu, Faliang An, Huajie Gu, and Fei Xu. "A novel aptasensor based on DNA hydrogel for sensitive visual detection of ochratoxin A." *Microchimica Acta* 188 (2021): 1-10.

(49) Ramachandran, Tholkappiyan, Ashraf Ali, Haider Butt, Lianxi Zheng, Firdous Ahmad Deader, and Moh'D. Rezeq. "Gold on the horizon: unveiling the chemistry, applications and future prospects of 2D monolayers of gold nanoparticles (Au-NPs)." *Nanoscale Advances* 6, no. 22 (2024): 5478-5510.

(50) Kumar, Yedluri Anil, Siva Sankar Sana, Tholkappiyan Ramachandran, Mohammed A. Assiri, Sunkara Srinivasa Rao, and Seong Cheol Kim. "From lab to field: Prussian blue frameworks as sustainable cathode materials." *Dalton*

Transactions 53, no. 26 (2024): 10770-10804.

View Article Online
DOI: 10.1039/D5TB00990A

View Article Online
DOI: 10.1039/D5TB00990A

Data availability statements

All data generated or analyzed during this study are included in this published article (and its supplementary information files).

Corresponding Author: Cheng-Hsin Chuang, 28th April, 2025